

Resolving CO₂ activation and hydrogenation pathways over iron carbides from DFT investigation

Xianglin Liu^a, Chenxi Cao^a, Pengfei Tian^a, Minghui Zhu^a, Yulong Zhang^a, Jing Xu^{a,*}, Yun Tian^b, Yi-Fan Han^{a,b,*}

^a State Key Laboratory of Chemical Engineering, East China University of Science and Technology, Shanghai, 200237, China

^b Engineering Research Center of Advanced Functional Material Manufacturing of Ministry of Education, Zhengzhou University, Zhengzhou, 450001, China



ARTICLE INFO

Keywords:
CO₂ activation
Hydrogenation
Iron carbides
Density functional theory
Reaction pathway

ABSTRACT

In this work, periodic density functional theory (DFT) calculations were performed to investigate the CO₂ activation mechanism over thermodynamically stable χ -Fe₅C₂ (510) and θ -Fe₃C (031) facets. Four major pathways of CO₂ activation were examined, including the direct dissociation of CO₂ and the H-assisted intermediates of *COOH, *HCOO, and *CO + *OH. Both χ -Fe₅C₂ and θ -Fe₃C have proven to be active for CO₂ direct dissociation ($E_a = 0.17$ eV). As for H assisted CO₂ activation, the one-step formation of *CO + *OH is feasible on χ -Fe₅C₂ ($E_a = 0.24$ eV). Furthermore, θ -Fe₃C favors the *HCOO pathway ($E_a = 0.20$ eV) and *CO + *OH formation ($E_a = 0.11$ eV), while neither phase favors the formation of *COOH. Both CO₂ direct activation and H-assisted CO₂ activation pathways are of vital importance under high ratio of H/C in CO₂ hydrogenation reaction. This work sheds light on CO₂ activation mechanism over iron carbides, improving the rational design of CO₂ hydrogenation catalysts.

1. Introduction

Mitigation of CO₂ concentration has become a great challenge since it has a strong impact on the globe climate change and the ocean acidification [1,2]. Catalytic hydrogenation of CO₂ has attracted more attention as a promising approach for the recycling of CO₂ into high-value-added chemicals [3–6]. In this respect, CO₂ is a plentiful and renewable C1 feedstock for the chemical production rather than a greenhouse gas.

Numerous efforts have been devoted to promote CO₂ hydrogenation to valuable chemicals, including methane, methanol, light olefins and heavier hydrocarbons [7–20]. CO₂ hydrogenation has been investigated over both noble metal catalysts [21–23] and non-noble metal catalysts [12,17,24–28]. Compared with other metal catalysts, Fe-based catalysts are more easily available and show excellent activity for both reverse water-gas shift (RWGS) and Fischer-tropsch synthesis (FTS) reactions, which allows CO₂ hydrogenation to occur in a cascade over a single catalyst [12,17,26–29]. It is well known that CO is produced mainly from CO₂ by RWGS over iron oxide phases, then reacts with H₂ to form hydrocarbons via (FTS) over iron carbides [12,16,29–32]. The structure of the FTS catalyst is too complex to understand the reaction mechanism in this catalytic system, especially in the initial step on how to

activate CO₂ molecule [20,27,33,34]. Due to only few techniques available for revealing the CO₂ activation, therefore, it is urgent to reveal the mechanism of CO₂ activation by theoretical calculation.

First-principles calculation, as a powerful tool for analyzing reaction pathways at the molecular level, has been extensively used to study CO₂ hydrogenation over Fe-based catalysts. Fe (110) and Fe (100) were found to favor the dissociation of CO₂ into *CO and *O, while the competitive formation of *CO and *HCOO also existed over Fe (211) [35]. Recently, Nie et al. [34] have studied CO₂ direct dissociation on Fe (100), χ -Fe₅C₂ (510) and Fe₃O₄ (111) facets. χ -Fe₅C₂ (510) surface showed the lowest dissociation energy barrier of 0.50 eV, while Fe₃O₄ (111) exhibited the highest barrier of over 2.0 eV. In addition, it's noted that H coverages were above 1.0 under the FTS conditions (H₂/CO = 10, 0.185 MPa) [36], therefore, the effect of atomic H on CO₂ activation pathways may play a vital role that features higher H₂ partial pressures (H₂/CO₂ ≥ 3, 1 ~ 2 MPa) under CO₂ hydrogenation conditions. There has been some study on CO₂ activation over certain iron-based catalyst, however, a comprehensive investigation of all possible CO₂ activation pathways including direct activation and H-assisted activation on iron carbides has not been reported yet.

In this work, periodic spin-polarized density functional theory (DFT) calculations were conducted to examine CO₂ activation mechanism

* Corresponding authors at: State Key Laboratory of Chemical Engineering, East China University of Science and Technology, Shanghai, 200237, China.

E-mail addresses: xujing@ecust.edu.cn (J. Xu), yifanhan@ecust.edu.cn (Y.-F. Han).

over a series of different Fe-based catalysts. Given the high ratio of H₂ to CO₂ used in CO₂ hydrogenation, four CO₂ activation pathways were considered:

- (i) *CO₂ → *CO + *O
- (ii) *CO₂ + *H → *COOH → *CO + *OH
- (iii) *CO₂ + *H → *HCOO → *HCO + *O
- (iv) *CO₂ + *H → *CO + *OH

2. Computational models

Bulk $\chi\text{-Fe}_5\text{C}_2$ and $\theta\text{-Fe}_3\text{C}$ exhibit monoclinic and orthorhombic crystal structures respectively (Fig. 1(a)). Both $\chi\text{-Fe}_5\text{C}_2$ (510) and $\theta\text{-Fe}_3\text{C}$ (031) facets belong to plate-like surface (Fig. S1), whereas the composition and arrangement of iron and carbon atoms exposed on the surface is different. All typical active sites for the two surfaces are marked in Fig. 1(b). For $\chi\text{-Fe}_5\text{C}_2$ (510) surface, the unit cell consists of ten top Fe sites (Fe^X), two top C sites (C_S^X), ten 3-fold hollow sites (3F^X) and three 4-fold hollow sites (4F^X); for $\theta\text{-Fe}_3\text{C}$ (031) surface, eight top Fe sites, one top C site, six 3-fold hollow sites and two 4-fold hollow sites are considered. Before the DFT calculations, the models and the parameters have been examined to ensure the reliability of calculation (Tables S1–S7).

3. Results and discussion

Adsorption of reactants (CO₂ and H₂) has a significant impact on subsequent surface reactions of CO₂ hydrogenation. The projected density of states (PDOS) of d-orbitals and the d-band center for the surface Fe atoms of $\chi\text{-Fe}_5\text{C}_2$ (510) and $\theta\text{-Fe}_3\text{C}$ (031) surfaces were first calculated (Fig. 1(c)) to provide insights into the formation and activation of chemical bonds between the adsorbate and the surface [37]. The d-band center for $\chi\text{-Fe}_5\text{C}_2$ (510) and $\theta\text{-Fe}_3\text{C}$ (031) surfaces are -0.84 eV and -1.11 eV, respectively. A downward shift of the d-band center relative to the Fermi level results in weakening of the binding strength because of increased occupation of empty antibonding orbitals

[38,39]. Therefore, $\chi\text{-Fe}_5\text{C}_2$ (510) surface is expected to favor the adsorption of reactant molecules.

3.1. CO₂ adsorption

CO₂ adsorption at all possible sites on the iron carbide surfaces were explored. In general, CO₂ tends to adsorb in a horizontal configuration with its carbon atom bonded with the surface Fe. On $\chi\text{-Fe}_5\text{C}_2$ (510) facet, among the four favorable CO₂ adsorption configurations (Fig. S2, Table S8), CO₂ adsorbed at the 3F⁵ site exhibits the lowest adsorption energy of -0.73 eV. The adsorption energy is not linearly correlated with the number of electrons transferred according to calculations of charge density differences and the Bader charge (Figs. S3 and S4(a)). The Bader charge for the most stable adsorbed-state CO₂ on $\chi\text{-Fe}_5\text{C}_2$ (510) surface is 0.63^{δ-} at the 3F⁵ site. In comparison, adsorbed H₂ molecule on $\chi\text{-Fe}_5\text{C}_2$ (510) surface is found to spontaneously dissociate without energy barrier. The binding energy of surface hydrogen is -1.33 eV, much stronger than that of CO₂ (Fig. S5(a)).

On $\theta\text{-Fe}_3\text{C}$ (031) facet, CO₂ adsorption at the 3F⁴ site is the most stable with an adsorption energy of -0.62 eV (Fig. S6, Table S9). The Bader charge of the most stable adsorbed CO₂ on $\theta\text{-Fe}_3\text{C}$ (031) surface is 0.76^{δ-}, which is also not the most negatively charged one on $\chi\text{-Fe}_5\text{C}_2$ (510) facet (Figs. S7 and S4(b)). So it can be interpreted as that, in addition to electron donation from the surface, the spatial effect such as local arrangement of surface atoms also plays an important role in stabilizing the adsorbed CO₂. Adsorbed H₂ molecules on $\theta\text{-Fe}_3\text{C}$ (031) surface are also ready to dissociate into surface hydrogen (Fig. S5(b)). The binding energy of -1.32 eV is similar to that on $\chi\text{-Fe}_5\text{C}_2$ (510) surface.

In addition, the adsorption properties of key intermediates, including COOH, HCOO, HCO and OH, have significant influences on the reaction, and even directly affect the reaction pathway. The adsorption properties of key intermediates (Table S10) show that the HCOO intermediate is more stable than COOH intermediate, indicating that the HCOO intermediate pathway is more favorable than the COOH pathway. Furthermore, there is no obvious correlation between the

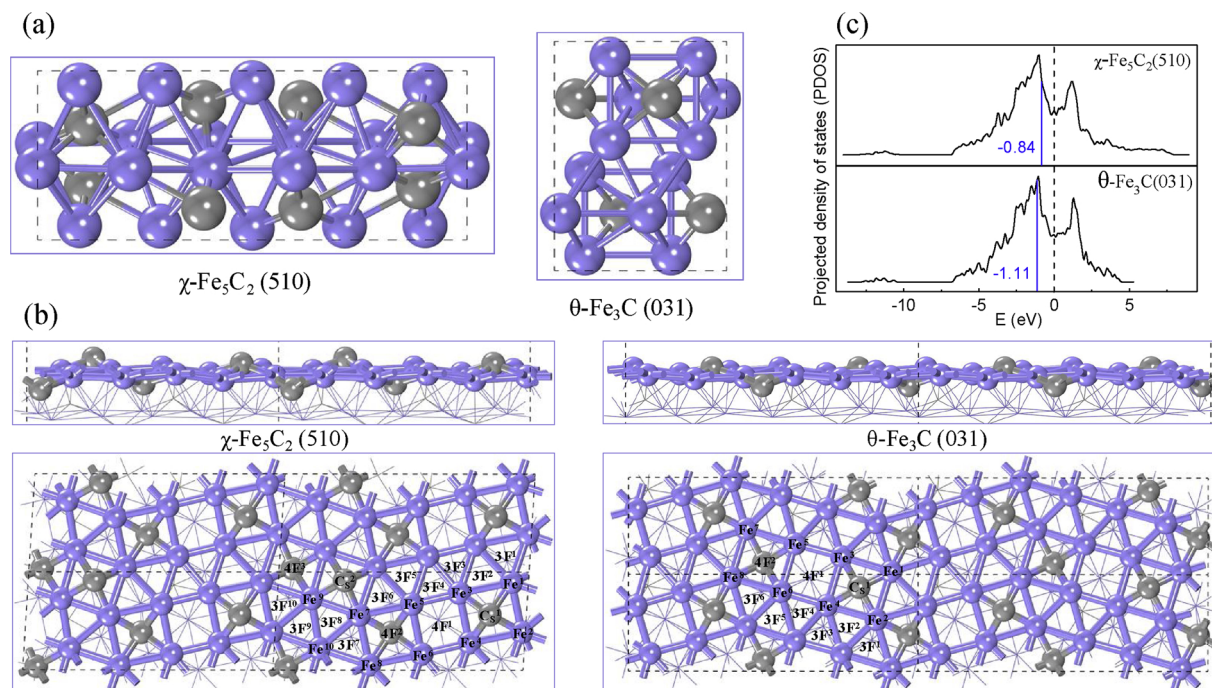
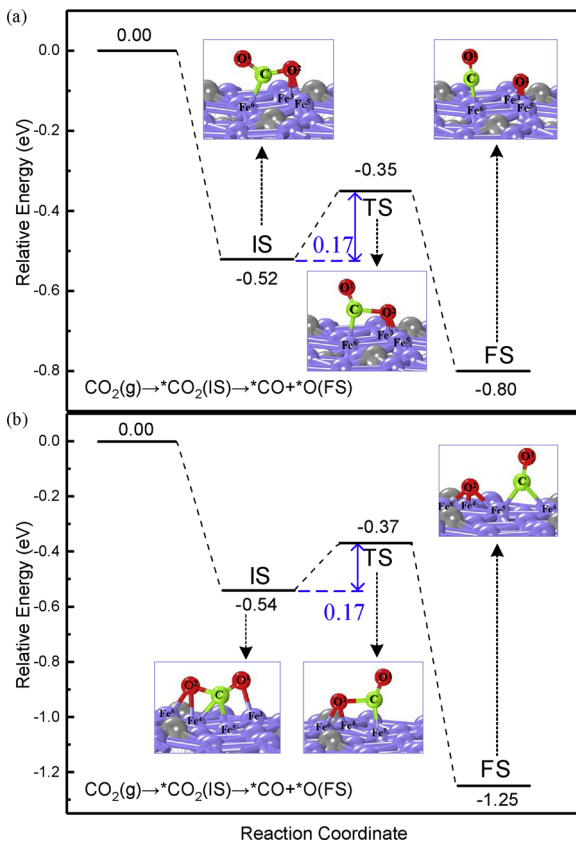


Fig. 1. (a) Geometric structures of $\chi\text{-Fe}_5\text{C}_2$ and $\theta\text{-Fe}_3\text{C}$ unit cells. (b) Side and top views of $\chi\text{-Fe}_5\text{C}_2$ (510) and $\theta\text{-Fe}_3\text{C}$ (031) surfaces. (Fe atoms in purple, C atoms in gray) (c) Projected density of states (PDOS) of the d-orbitals of the surface Fe atoms for $\chi\text{-Fe}_5\text{C}_2$ (510) and $\theta\text{-Fe}_3\text{C}$ (031) surfaces. The vertical black dashed lines represent the d-band center and the vertical blue lines indicate the d-band center.



adsorption energy and the charge transfer or the adsorption configurations.

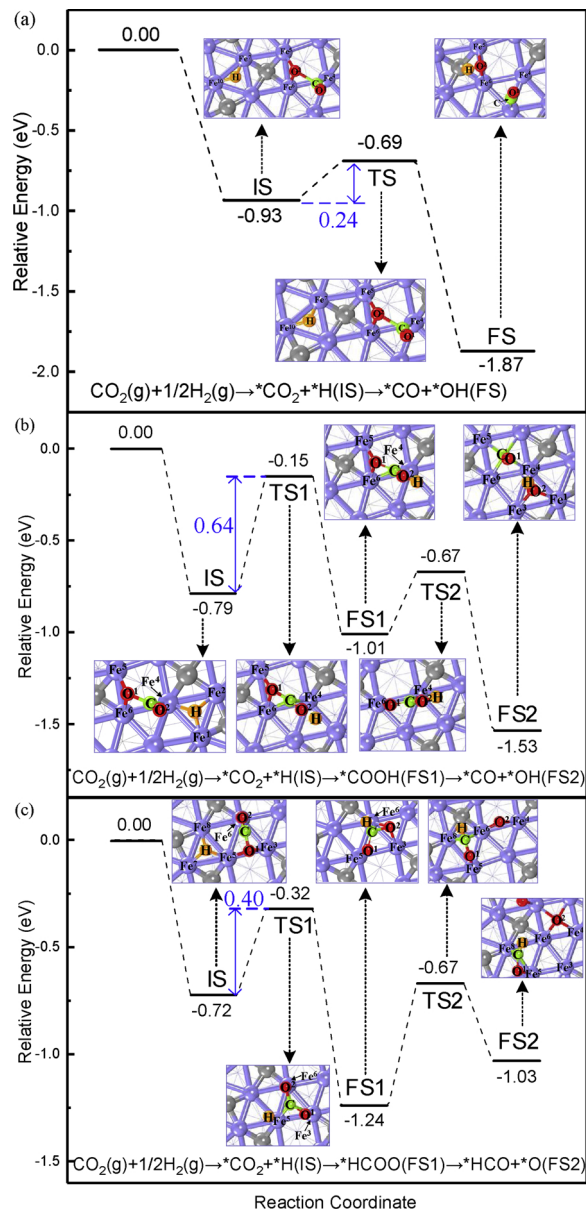
3.2. CO₂ direct dissociation

The dissociation of adsorbed CO₂ into *CO and *O was examined on the basis of stable CO₂ adsorption configurations over $\chi\text{-Fe}_5\text{C}_2$ (510) and $\theta\text{-Fe}_3\text{C}$ (031) surfaces in order to understand the direct dissociation pathway of *CO₂. On $\chi\text{-Fe}_5\text{C}_2$ (510) facet (Fig. S8, Table S11), the most stable adsorbed state CO₂ has a dissociation energy barrier of 0.41 eV. However, CO₂ adsorption at 3F⁴ (Fig. S2(a)), which is not the most stable adsorption configuration, shows the lowest dissociation barrier of only 0.17 eV (Fig. 2(a)). The reaction energy is -0.28 eV (exothermic).

On $\theta\text{-Fe}_3\text{C}$ (031) facet (Fig. S9, Table S12), the most stable adsorbed-state CO₂ at the 3F⁴ site has a barrier of 0.25 eV for direct dissociation. While CO₂ adsorbed at the 3F³ site exhibits the lowest dissociation energy barrier of only 0.17 eV (Fig. 2(b)), which is the same as that on $\chi\text{-Fe}_5\text{C}_2$ (510). The reaction energy is -0.71 eV (exothermic), which is larger than that on $\chi\text{-Fe}_5\text{C}_2$ (510).

3.3. H-assisted CO₂ dissociation

Additionally, prompt dissociation of molecular H₂ on the iron carbide surfaces provides abundant active surface H atoms to allow for H assisted CO₂ dissociation. H assisted CO₂ dissociation includes three pathways, namely the *CO + *OH, *COOH and *HCOO pathways, depending on whether *H attacks the C or O atom; *HCOO or *COOH could further dissociate into *HCO and *O or *CO and *OH. Based on the stable CO₂ adsorption configurations, we first screened out favorable co-adsorption structures of *CO₂ and *H as the IS on $\chi\text{-Fe}_5\text{C}_2$ (510)



facet. Then, typical CO₂ activation pathways with H assistance were considered (Figs. S10–S12, Table S11). The profiles with the lowest energy barrier and optimized structures of each pathway are illustrated in Fig. 3.

Among all H-assisted pathways, the *COOH route exhibits higher activation barriers of no less than 0.64 eV (corresponding to the Fe⁴ site) regardless of the adsorption site. The *HCOO pathway also shows relatively high energy barriers, with the lowest energy barrier of 0.40 eV corresponding to the 3F⁴ site. By contrast, *CO and *OH formation in one step at the Fe⁴ site has the lowest dissociation barrier of 0.24 eV. The reaction energy is -0.94 eV (exothermic).

*CO₂ activation with H assistance on $\theta\text{-Fe}_3\text{C}$ (031) facet was also studied and compared with that on $\chi\text{-Fe}_5\text{C}_2$ (510) facet (Figs. S13–S15, Table S12). Among all the calculated pathways, the *COOH pathway shows a high activation barrier of 1.00 eV at the 3F⁵ site (Fig. 4). The *CO and *OH formation in one step shows an extremely low energy barrier of 0.11 eV at the 3F³ site. The reaction energy is -1.08 eV, i.e.,

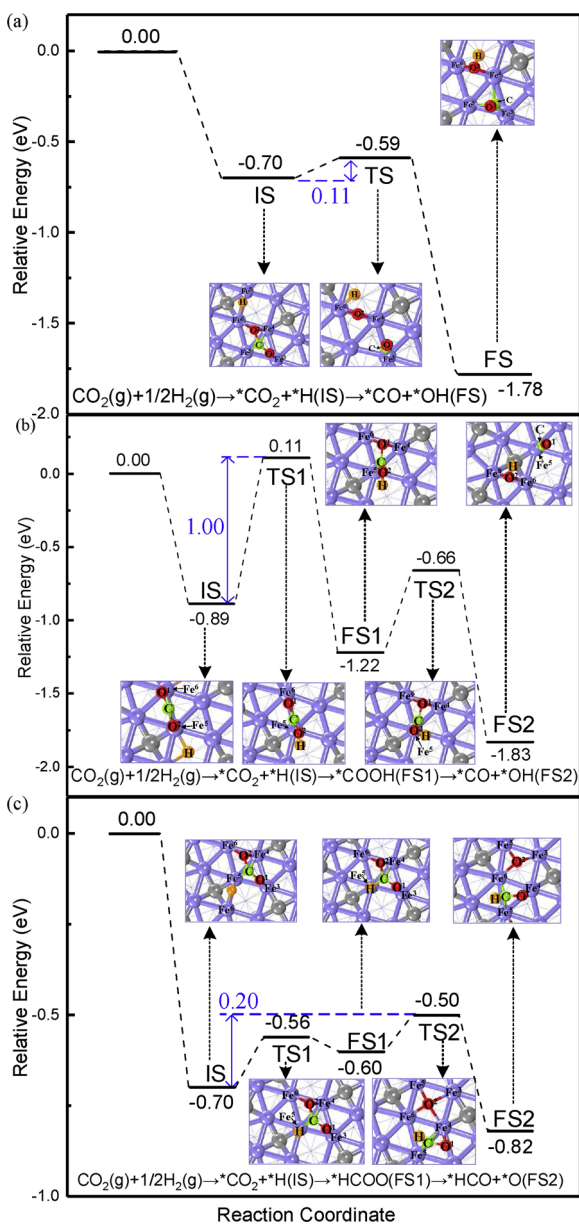


Fig. 4. Potential energy profiles of CO₂ activation with H assistance in pathways of *CO and *OH, *COOH and *HCOO intermediates on $\theta\text{-Fe}_3\text{C}$ (031) surface. (Fe atoms in purple, C atoms of $\theta\text{-Fe}_3\text{C}$ (031) in gray, C atoms of CO₂ in green, O atoms of CO₂ in red, H atoms in orange.).

the reaction energy is more exothermic than that on $\chi\text{-Fe}_5\text{C}_2$ (510) facet. *HCOO intermediate pathway also exhibits lower energy barrier of 0.20 eV at the 3F³ site. The whole process is exothermic by 0.12 eV, which is lower than the *CO and *OH pathway. All the

3.4. Discussion

Several iron phases were previously observed during CO and CO₂ hydrogenation reaction [9,33,40,41], including metallic iron, magnetite and iron carbides. Among them, $\chi\text{-Fe}_5\text{C}_2$ and $\theta\text{-Fe}_3\text{C}$ are the most abundant iron carbide species confirmed by experiments [9,42–45].

3.4.1. CO₂ adsorption

The adsorption energy and activation barriers of CO₂ over $\chi\text{-Fe}_5\text{C}_2$ (510), $\theta\text{-Fe}_3\text{C}$ (031), tet1-Fe₃O₄ (111), oct2-Fe₃O₄ (111), Fe (100), Fe (110), Fe (111), as well as those over Fe (211), are summarized (Fig. 5). Our calculations clearly indicate considerable adsorption strength of

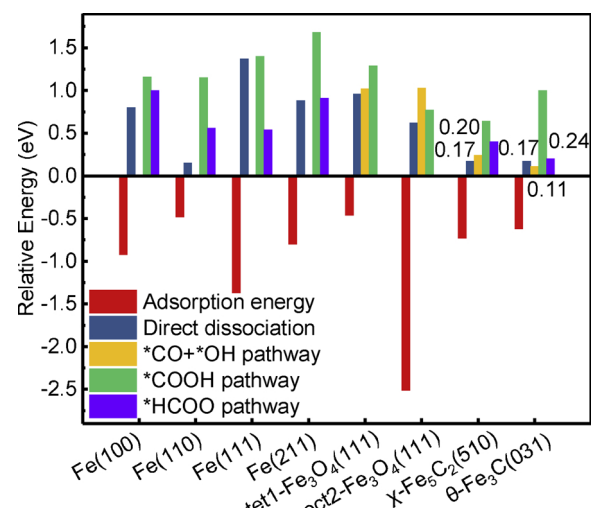


Fig. 5. CO₂ adsorption and activation energies on metallic iron, magnetite and iron carbides surfaces [26,34,35].

CO₂ on both $\chi\text{-Fe}_5\text{C}_2$ (510) and $\theta\text{-Fe}_3\text{C}$ (031) surfaces, given adsorption energies as high as -0.73 eV. In comparison, the adsorption energy of CO₂ on tet1-terminated and oct2-terminated Fe₃O₄ (111) surfaces are reported to be -0.46 eV [34]/-0.43 eV [46] and -2.51 eV [34], respectively. The classical Sabatier principle states that there is an optimum “bond strength” defining the catalyst activity for a given reaction. Compared with iron and magnetite, the adsorption strength of CO₂ on iron carbides might be appropriate for activation.

3.4.2. CO₂ direct activation

The activation energy barriers of CO₂ direct dissociation on tet1-terminated and oct2-terminated Fe₃O₄ (111) surfaces are as high as 0.96 and 0.62 eV, respectively [26]. While the CO₂ direct dissociation is much more favorable on $\chi\text{-Fe}_5\text{C}_2$ (510) and $\theta\text{-Fe}_3\text{C}$ (031) facets with an energy barrier of 0.17 eV. It worth mentioning that the CO₂ direct dissociation barrier is 0.15 eV on Fe (110) surface [35]. So we expect that iron carbides and metallic iron are more effective in catalytic CO₂ activation than its oxides, which is the generally accepted active phase of RWGS [47]. Besides, metallic iron is unstable under the reaction conditions of CO₂ hydrogenation and prone to carbonization to carbides quickly [9,48]. Hence, CO₂ direct dissociation over Hägg carbide and cementite is more feasible.

3.4.3. H-assisted CO₂ activation

As previously explained, H-assisted CO₂ activation pathways are dominating. Facilitated by surface H atoms, *CO₂ dissociation to *CO and *OH in one step is favorable on both $\chi\text{-Fe}_5\text{C}_2$ (510) and $\theta\text{-Fe}_3\text{C}$ (031) surfaces with energy barriers of 0.24 eV and 0.11 eV, respectively. However, on tet1-terminated and oct2-terminated Fe₃O₄ (111) surfaces [26], the *CO and *OH pathways are not preferred because the activation barriers are both larger than 1.00 eV. Meanwhile, *CO₂ activation via dissociation of the *HCOO is also favorable over $\theta\text{-Fe}_3\text{C}$ (031) given the barrier of 0.20 eV, which is comparable with the *CO and *OH pathway. In contrast, *HCOO formation energy barrier are all over 0.50 eV on metallic iron surfaces. In summary, the H-assisted *COOH pathways are relatively unfavorable on all the facets due to higher energy barriers. Therefore, in comparison to metallic iron and magnetite, iron carbides are more prone to activate CO₂ with assistance of H atom under CO₂ hydrogenation conditions.

3.4.4. CO₂ activation under typical CO₂ hydrogenation conditions

Our findings bring new insights for understanding the mechanism of CO₂ hydrogenation over iron-based catalysts. It is well known that iron carbides (mainly $\chi\text{-Fe}_5\text{C}_2$ and $\theta\text{-Fe}_3\text{C}$) and oxide (mainly Fe₃O₄) are the

dominant phases in iron based CO₂ hydrogenation catalysts [8,10,49]. Based on our previous experimental results [9], we calculated the reaction rate normalized by the data obtained from nitrogen physical adsorption and XPS characterization. Iron carbides show higher activity than Fe₃O₄ (Table S21), in good agreement with the DFT results. Dynamic interconversion between surface phases readily occurs during the reaction controlled by the balance between reducing agent (H₂) and oxidation agent (CO₂, H₂O) in the atmosphere [27,48,50]. Previous work has underscored the high RWGS catalytic activity of magnetite [47,51]. However, given the facile activation of CO₂ on iron carbides as demonstrated in this work, we believe that iron carbides are responsible for the initial activation of CO₂, while the exact role of iron carbides and oxides during the reaction is unsettled and entails further elaboration. We expect that magnetite is responsible for CO₂ adsorption, while CO₂ activation mainly occurs on the iron carbides. In addition, we have demonstrated that surface adsorbed H atoms have a significant effect on the CO₂ activation pathways as well as the resulted surface reactive intermediates. Under CO₂ hydrogenation condition, the adsorption energy of H₂ is much higher than that of CO₂. So H-assisted CO₂ activation pathways may dominate under high H coverage due to the competitive adsorption of H₂ and CO₂ [36]. CO₂ adsorption may be a decisive step on iron carbides. Therefore, we suggest adding some alkali metal additives to regulate the competitive adsorption of CO₂ and H₂, so as to control the reactivity and selectivity.

4. Conclusion

To summarize, CO₂ adsorption and activation mechanism over metallic iron, magnetite and iron carbides have been investigated comprehensively. Despite the weak interactions with many metal surfaces, CO₂ adsorption is facile on both iron carbide surfaces to drive subsequent activation of CO₂. CO₂ direct dissociation to *CO and *O is favorable on χ -Fe₅C₂ and θ -Fe₃C. Furthermore, H-assisted pathways exist in parallel, *CO and OH formation in one step on two iron carbides and *HCOO route over θ -Fe₃C are competitive CO₂ activation pathways. However, neither facet favors the formation of *COOH intermediate. Both χ -Fe₅C₂ and θ -Fe₃C are promising candidates for direct CO₂ dissociation and hydrogenation with lower activation barriers compared to metallic iron and magnetite. The H-rich scenario adopted in our study better reflects the practical reaction conditions and should also be considered in the evaluation of subsequent reaction steps. The superior intrinsic activity of iron carbides to magnetite in CO₂ activation and hydrogenation under typical reaction conditions might inspire future catalyst designs focusing on enhancement of co-adsorption of hydrogen and CO₂ and stabilization of the iron carbide phases under realistic reaction conditions. These new insights revealed in the work are expected to inspire the rational design of Fe-based catalysts for CO₂ hydrogenation reactions.

CRediT authorship contribution statement

Xianglin Liu: Conceptualization, Investigation, Methodology, Validation, Data curation, Writing - original draft, Writing - review & editing. **Chenxi Cao:** Writing - review & editing. **Pengfei Tian:** Methodology. **Minghui Zhu:** Writing - review & editing. **Yulong Zhang:** Investigation. **Jing Xu:** Supervision, Project administration, Writing - review & editing. **Yun Tian:** Writing - review & editing. **Yi-Fan Han:** Supervision, Writing - review & editing.

Declaration of Competing Interest

The authors declare that they have no known competing financial interests or personal relationships that could have appeared to influence the work reported in this paper.

Acknowledgements

This work was supported by the National Key R&D Program of China (2018YFB0605803), National Science Foundation (21878080 and 21808058), Shanghai Sailing Program (18YF1406100), Fundamental Research Funds for the Central Universities (222201718002 and 222201814006).

Appendix A. Supplementary data

Supplementary material related to this article can be found, in the online version, at doi:<https://doi.org/10.1016/j.jcou.2019.12.014>.

References

- [1] D.J. Arent, A. Wise, R. Gelman, The status and prospects of renewable energy for combating global warming, *Energ. Econ.* 33 (2011) 584–593.
- [2] R. Knutti, J. Rogelj, The legacy of our CO₂ emissions: a clash of scientific facts, politics and ethics, *Clim. Change* 133 (2015) 361–373.
- [3] T. Sakakura, J.-C. Choi, H. Yasuda, Transformation of carbon dioxide, *Chem. Rev.* 107 (2007) 2365–2387.
- [4] A. Otto, T. Grube, S. Schiebahn, D. Stolten, Closing the loop: captured CO₂ as a feedstock in the chemical industry, *Energy Environ. Sci.* 8 (2015) 3283–3297.
- [5] R.W. Dorner, D.R. Hardy, F.W. Williams, H.D. Willauer, Heterogeneous catalytic CO₂ conversion to value-added hydrocarbons, *Energy Environ. Sci.* 3 (2010) 884–890.
- [6] N. Mac Dowell, P.S. Fennell, N. Shah, G.C. Maitland, The role of CO₂ capture and utilization in mitigating climate change, *Nat. Clim. Change* 7 (2017) 243.
- [7] J. Liu, A. Zhang, X. Jiang, M. Liu, Y. Sun, C. Song, X. Guo, Selective CO₂ hydrogenation to hydrocarbons on Cu-promoted Fe-based catalysts: dependence on Cu-Fe interaction, *ACS Sustain. Chem. Eng.* 6 (2018) 10182–10190.
- [8] L. Guo, J. Sun, X. Ji, J. Wei, Z. Wen, R. Yao, H. Xu, Q. Ge, Directly converting carbon dioxide to linear α -olefins on bio-promoted catalysts, *Commun. Chem. Int.* 1 (2018) 11.
- [9] Y. Zhang, D. Fu, X. Liu, Z. Zhang, C. Zhang, B. Shi, J. Xu, Y.-F. Han, Operando spectroscopic study of dynamic structure of iron oxide catalysts during CO₂ hydrogenation, *ChemCatChem* 10 (2017) 1272–1276.
- [10] J. Wei, Q. Ge, R. Yao, Z. Wen, C. Fang, L. Guo, H. Xu, J. Sun, Directly converting CO₂ into a gasoline fuel, *Nat. Commun.* 8 (2017) 15174.
- [11] M.V. Landau, N. Meiri, N. Utsis, R. Vidruk Nehemya, M. Herskowitz, Conversion of CO₂, CO, and H₂ in CO₂ hydrogenation to fungible liquid fuels on Fe-based catalysts, *Ind. Eng. Chem. Res.* 56 (2017) 13334–13355.
- [12] M. Amoyal, R. Vidruk-Nehemya, M.V. Landau, M. Herskowitz, Effect of potassium on the active phases of Fe catalysts for carbon dioxide conversion to liquid fuels through hydrogenation, *J. Catal.* 348 (2017) 29–39.
- [13] R. Satthawong, N. Koizumi, C. Song, P. Prasasarakich, Light olefin synthesis from CO₂ hydrogenation over K-promoted Fe-Co bimetallic catalysts, *Catal. Today* 251 (2015) 34–40.
- [14] V. Landau Miron, R. Vidruk, M. Herskowitz, Sustainable production of green feed from carbon dioxide and hydrogen, *ChemSusChem* 7 (2014) 785–794.
- [15] P. Gao, S. Li, X. Bu, S. Dang, Z. Liu, H. Wang, L. Zhong, M. Qiu, C. Yang, J. Cai, W. Wei, Y. Sun, Direct conversion of CO₂ into liquid fuels with high selectivity over a bifunctional catalyst, *Nat. Chem.* 9 (2017) 1019.
- [16] W. Wang, S. Wang, X. Ma, J. Gong, Recent advances in catalytic hydrogenation of carbon dioxide, *Chem. Soc. Rev.* 40 (2011) 3703–3727.
- [17] X. Wang, G. Yang, J. Zhang, S. Chen, Y. Wu, Q. Zhang, J. Wang, Y. Han, Y. Tan, Synthesis of isooalkanes over a core (Fe-Zn-Zr)-shell (zeolite) catalyst by CO₂ hydrogenation, *Chem. Commun.* 52 (2016) 7352–7355.
- [18] A. Burchard, M.R. Kember, K.G. Sandeman, C.K. Williams, A bimetallic iron(III) catalyst for CO₂/epoxide coupling, *Chem. Commun.* 47 (2011) 212–214.
- [19] P. Gao, S. Dang, S. Li, X. Bu, Z. Liu, M. Qiu, C. Yang, H. Wang, L. Zhong, Y. Han, Q. Liu, W. Wei, Y. Sun, Direct production of lower olefins from CO₂ conversion via bifunctional catalysis, *ACS Catal.* 8 (2018) 571–578.
- [20] S. Saeidi, S. Najari, F. Fazlollahi, M.K. Nikoo, F. Sefidkon, J.J. Kleméš, L.L. Baxter, Mechanisms and kinetics of CO₂ hydrogenation to value-added products: a detailed review on current status and future trends, *Renew. Sust. Energ. Rev.* 80 (2017) 1292–1311.
- [21] H. Bahrui, M. Bowker, G. Hutchings, N. Dimitratos, P. Wells, E. Gibson, W. Jones, C. Brookes, D. Morgan, G. Lalev, Pd/ZnO catalysts for direct CO₂ hydrogenation to methanol, *J. Catal.* 343 (2016) 133–146.
- [22] Y. Hartadi, D. Widmann, R.J. Behm, CO₂ hydrogenation to methanol on supported Au catalysts under moderate reaction conditions: support and particle size effects, *ChemSusChem* 8 (2014) 456–465.
- [23] A.M. Abdel-Mageed, S. Eckle, D. Widmann, R.J. Behm, Water assisted dispersion of Ru nanoparticles: the impact of water on the activity and selectivity of supported Ru catalysts during the selective methanation of CO in CO₂-rich reformate, *J. Catal.* 335 (2016) 79–94.
- [24] G. Zhou, H. Liu, K. Cui, A. Jia, G. Hu, Z. Jiao, Y. Liu, X. Zhang, Role of surface Ni and Ce species of Ni/CeO₂ catalyst in CO₂ methanation, *Appl. Surf. Sci.* 383 (2016) 248–252.
- [25] J. Ye, C. Liu, D. Mei, Q. Ge, Active oxygen vacancy site for methanol synthesis from

- CO₂ hydrogenation on In₂O₃(110): a DFT study, *ACS Catal.* 3 (2013) 1296–1306.
- [26] L. Huang, B. Han, Q. Zhang, M. Fan, H. Cheng, Mechanistic study on water gas shift reaction on the Fe₃O₄ (111) reconstructed surface, *J. Phys. Chem. C* 119 (2015) 28934–28945.
- [27] E. de Smit, F. Cinquini, A.M. Beale, O.V. Safonova, W. van Beek, P. Sautet, B.M. Weckhuysen, Stability and reactivity of ϵ – χ – θ iron carbide catalyst phases in Fischer–Tropsch synthesis: controlling μ_c , *J. Am. Chem. Soc.* 132 (2010) 14928–14941.
- [28] H.M. Torres Galvis, J.H. Bitter, C.B. Khare, M. Ruitenberg, A.I. Dugulan, K.P. de Jong, Supported iron nanoparticles as catalysts for sustainable production of lower olefins, *Science* 335 (2012) 835.
- [29] T. Riedel, H. Schulz, G. Schaub, K.-W. Jun, J.-S. Hwang, K.-W. Lee, Fischer–tropsch on iron with H₂/CO and H₂/CO₂ as synthesis gases: the episodes of formation of the Fischer–tropsch regime and construction of the catalyst, *Top. Catal.* 26 (2003) 41–54.
- [30] N. Utsis, R. Vidruk-Nehemya, M.V. Landau, M. Herskowitz, Novel bifunctional catalysts based on crystalline multi-oxide matrices containing iron ions for CO₂ hydrogenation to liquid fuels and chemicals, *Faraday Discuss.* 188 (2016) 545–563.
- [31] X. Cui, P. Gao, S. Li, C. Yang, Z. Liu, H. Wang, L. Zhong, Y. Sun, Selective production of aromatics directly from carbon dioxide hydrogenation, *ACS Catal.* 9 (2019) 3866–3876.
- [32] B. Liang, H. Duan, T. Sun, J. Ma, X. Liu, J. Xu, X. Su, Y. Huang, T. Zhang, Effect of Na promoter on Fe-based catalyst for CO₂ hydrogenation to alkenes, *ACS sustain. Chem. Eng.* 7 (2019) 925–932.
- [33] L. Niu, X. Liu, X. Liu, Z. Lv, C. Zhang, X. Wen, Y. Yang, Y. Li, J. Xu, In situ XRD study on promotion effect of potassium on carburation of spray-dried precipitated Fe₂O₃ catalysts, *ChemCatChem* 9 (2017) 1691–1700.
- [34] X. Nie, L. Meng, H. Wang, Y. Chen, X. Guo, C. Song, DFT insight into the effect of potassium on the adsorption, activation and dissociation of CO₂ over Fe-based catalysts, *Phys. Chem. Chem. Phys.* 20 (2018) 14694–14707.
- [35] H. Wang, X. Nie, Y. Chen, X. Guo, C. Song, Facet effect on CO₂ adsorption, dissociation and hydrogenation over Fe catalysts: insight from DFT, *J. CO₂ Util.* 26 (2018) 160–170.
- [36] J. Xie, J. Yang, A.I. Dugulan, A. Holmen, D. Chen, K.P. de Jong, M.J. Louwerse, Size and promoter effects in supported iron Fischer–tropsch catalysts: insights from experiment and theory, *ACS Catal.* 6 (2016) 3147–3157.
- [37] B. Hammer, J.K. Nørskov, Electronic factors determining the reactivity of metal surfaces, *Surf. Sci.* 343 (1995) 211–220.
- [38] S.D. Miller, J.R. Kitchin, Relating the coverage dependence of oxygen adsorption on Au and Pt fcc(111) surfaces through adsorbate-induced surface electronic structure effects, *Surf. Sci.* 603 (2009) 794–801.
- [39] J.R. Kitchin, J.K. Nørskov, M.A. Bartaeu, J.G. Chen, Role of strain and ligand effects in the modification of the electronic and chemical properties of bimetallic surfaces, *Phys. Rev. Lett.* 93 (2004) 156801.
- [40] S. Saeidi, N.A.S. Amin, M.R. Rahimpour, Hydrogenation of CO₂ to value-added products—a review and potential future developments, *J. CO₂ Util.* 5 (2014) 66–81.
- [41] C.G. Visconti, M. Martinelli, L. Falbo, L. Fratalocchi, L. Lietti, CO₂ hydrogenation to hydrocarbons over Co and Fe-based Fischer-Tropsch catalysts, *Catal. Today* 277 (2016) 161–170.
- [42] T. Herranz, S. Rojas, F.J. Pérez-Alonso, M. Ojeda, P. Terreros, J.L.G. Fierro, Genesis of iron carbides and their role in the synthesis of hydrocarbons from synthesis gas, *J. Catal.* 243 (2006) 199–211.
- [43] J.W. Niemantsverdriet, A.M. Van der Kraan, W.N. Delgass, M.A. Vannice, Small-particle effects in Moessbauer spectra of a carbon-supported iron catalyst, *J. Phys. Chem.* 89 (1985) 67–72.
- [44] C. Yang, H. Zhao, Y. Hou, D. Ma, Fe₅C₂ nanoparticles: a facile bromide-induced synthesis and as an active phase for Fischer–Tropsch synthesis, *J. Am. Chem. Soc.* 134 (2012) 15814–15821.
- [45] B. Chen, D. Wang, X. Duan, W. Liu, Y. Li, G. Qian, W. Yuan, A. Holmen, X. Zhou, D. Chen, Charge-tuned CO activation over a χ -Fe₅C₂ Fischer–Tropsch catalyst, *ACS Catal.* 8 (2018) 2709–2714.
- [46] T. Su, Z. Qin, G. Huang, H. Ji, Y. Jiang, J. Chen, Density functional theory study on the interaction of CO₂ with Fe₃O₄(111) surface, *Appl. Surf. Sci.* 378 (2016) 270–276.
- [47] M. Zhu, T.C.R. Rocha, T. Lunkenbein, A. Knop-Gericke, R. Schlögl, I.E. Wachs, Promotion mechanisms of iron oxide-based high temperature water–gas shift catalysts by chromium and copper, *ACS Catal.* 6 (2016) 4455–4464.
- [48] Y.H. Choi, E.C. Ra, E.H. Kim, K.Y. Kim, Y.J. Jang, K.-N. Kang, S.H. Choi, J.-H. Jang, J.S. Lee, Sodium-containing spinel zinc ferrite as catalyst precursor for the selective synthesis of liquid hydrocarbon fuels, *ChemSusChem* 10 (2017) 4764–4770.
- [49] I.D. Gonzalez-Jimenez, K. Cats, T. Davidian, M. Ruitenberg, F. Meirer, Y. Liu, J. Nelson, J.C. Andrews, P. Pianetta, F.M.F. de Groot, B.M. Weckhuysen, Hard x-ray nanotomography of catalytic solids at work, *Angew. Chem. Int. Ed.* 51 (2012) 11986–11990.
- [50] E. de Smit, M.M. van Schooneveld, F. Cinquini, H. Bluhm, P. Sautet, F.M.F. de Groot, B.M. Weckhuysen, On the surface chemistry of iron oxides in reactive gas atmospheres, *Angew. Chem. Int. Ed.* 50 (2011) 1584–1588.
- [51] F. Polo-Garzon, V. Fung, L. Nguyen, Y. Tang, F. Tao, Y. Cheng, L.L. Daemen, A.J. Ramirez-Cuesta, G.S. Foo, M. Zhu, I.E. Wachs, D.-e. Jiang, Z. Wu, Elucidation of the reaction mechanism for high-temperature water gas shift over an industrial-type copper–chromium–iron oxide catalyst, *J. Am. Chem. Soc.* 141 (2019) 7990–7999.